

# Transient Heat Transfer Model for Car Body Primer Curing

D. Zabala, N. Sánchez and J. Pinto

**Abstract**—A transient heat transfer mathematical model for the prediction of temperature distribution in the car body during primer baking has been developed by considering the thermal radiation and convection in the furnace chamber and transient heat conduction governing equations in the car framework. The car cockpit is considered like a structure with six flat plates, four vertical plates representing the car doors and the rear and front panels. The other two flat plates are the car roof and floor. The transient heat conduction in each flat plate is modeled by the lumped capacitance method. Comparison with the experimental data shows that the heat transfer model works well for the prediction of thermal behavior of the car body in the curing furnace, with deviations below 5%.

**Keywords**—Transient heat transfer, car body, lumped capacitance, primer baking.

## I. INTRODUCTION

HEAT transfer modeling in furnaces is a matter of interest in different material science applications [1]-[9] and in automotive industry. In this one, corrosion protection is a major concern during the car body assembly. In some process, heating of the car body is needed after the electro-deposition primer application because it is necessary to achieve a prescribed temperature/time range for proper primer curing or baking. Below that range, the polymerization of the resin is incomplete, and the primer will separate from the car surface and above it, the primer will be burned, affecting the final car painting, producing changes in pigmentation and damaging the resin of the primer, resulting in poor adhesion of following paint layers. Due to the temperature in the furnace chamber, radiation and convection are the modes of heat transfer from the furnace to the car structure. In order to design a new furnace or to improve the performance of existing ones, the modeling of the heat transfer process has to be done accurately.

D. Zabala is professor at the Universidad de Carabobo (CIMEC), Carabobo, Venezuela (corresponding author phone: 58-241-6005000 ext 305210; e-mail: dzabala@uc.edu.ve).

N. Sánchez, was student at Universidad de Carabobo, Carabobo, Venezuela. Recently he worked for Moseinca (e-mail: nelsondavid44@hotmail.com).

J. Pinto was student at Universidad de Carabobo, Carabobo, Venezuela. He is now Business Development Engineer at Kraft Foods Venezuela (e-mail: jesus-pinto@hotmail.com).

## II. MATHEMATICAL MODEL

### A. Energy Balance in car body

The car cockpit is considered like a structure with six flat plates, four vertical plates representing the car doors and the rear and front panels. The other two flat plates are the car roof and floor. The transient heat conduction in each flat plate is modeled by the lumped capacitance method. Fig.1 shows the energy balance done in each panel of the car body. Radiation is considered to be added to the panel from the furnace walls ( $Q_{rs}$ ), the other surrounding panels ( $Q_{rop}$ ) and from the gases inside ( $Q_{ri}$ ) and outside ( $Q_{re}$ ) the car body. Also, emitted radiation ( $Q_{rE}$ ) from the panel is considered. Convection is considered from the gases inside ( $Q_{ci}$ ) and outside ( $Q_{ce}$ ) the car body.

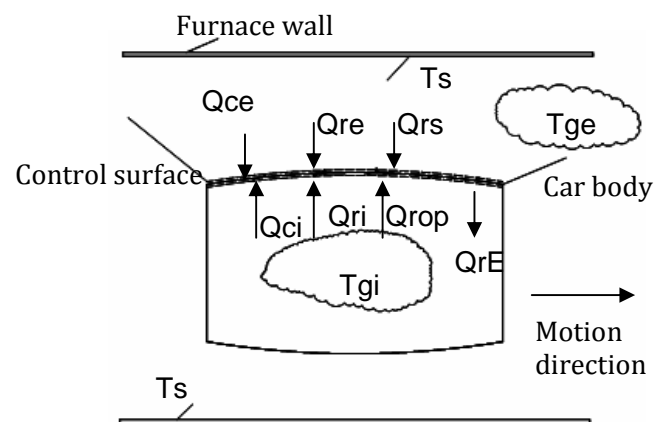


Fig. 1. Energy balance in left side panel

From the Fig. 1, the energy balance for each flat plate “i” is shown in (1):

$$\frac{dE}{dt} = Q_{re} + Q_{ri} + Q_{rs} + Q_{rop} + Q_{ce} + Q_{ci} - Q_{rE} \quad (1)$$

Equation (1) is transformed to (2), in terms of temperature if the lumped capacitance method is valid. This condition is verified by calculation of the Biot number for the car body, as in (3).

$$\rho_a e_i C_a \frac{dT_i}{dt} = \sigma \alpha (T_{ge}^4 + T_{gi}^4 + T_s^4) + h_{ex} (T_{ge} - T_i) \quad (2)$$

$$+ h_{in} (T_{gi} - T_i) + \sigma \alpha \sum_{j=1, j \neq i}^6 T_j^4 - \sigma \epsilon T_i^4$$

$$Bi = \frac{hL_c}{k} \quad (3)$$

Where the characteristic length  $L_c$  is defined as the ratio between the car body volume and surface area,  $k$  is the metal thermal conductivity and  $h$  is the convection heat transfer coefficient. For each flat plate,  $L_c$  is defined according the flat plate orientation. Each flat plate "i" is represented by (2), and then the theoretical car body temperature distribution is obtained by solving the system of six coupled ordinary differential equations. These predicted temperatures are compared with the experimental temperatures obtained by the thermocouples attached to the car body. In figure 2, there is an example of the experimental car body temperature measured in different thermocouple locations. The measurement system records the temperature values, so these values were used for comparison with the predicted ones.

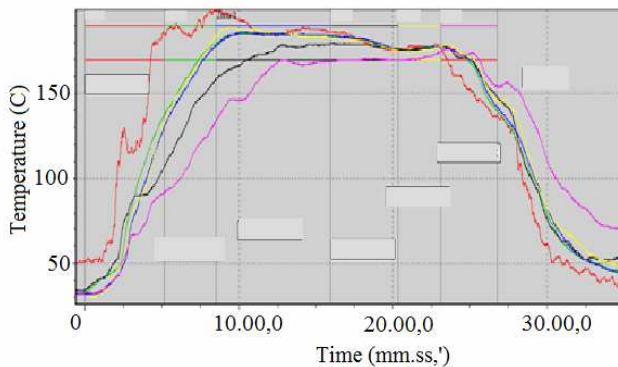


Fig. 2. Car body temperature experimental curves

### B. Convection heat transfer coefficients

The convection heat transfer mode inside the furnace is primarily by the diffusion mechanism or natural convection.

Due to the selected structure for the car body parts, two different convection coefficients must be calculated, for vertical and horizontal flat plates. Because the temperature of gas inside the car body is changing during the time, together with the car body temperature, average convection coefficients must be calculated by different average film temperature ( $T_f$ ). In this way, we obtain convection coefficients,  $h_{ex}$  and  $h_{in}$  as temperature dependant functions.

#### Vertical flat plates:

Churchill and Chu correlation [10] can be used for calculation of average Nusselt number (4), valid over the entire range of the Rayleigh number ( $Ra_L$ ) and depending on the Prandtl number. Also, the Warner and Arpaci correlation

[11], shown in (5), can be used for Nusselt number calculation.

$$Nu_L = \left[ 0.825 + \frac{0.387 (Ra_L)^{1/4}}{\left( 1 + \left( \frac{0.492}{Pr} \right)^{1/4} \right)^{4/7}} \right]^2 \quad (4)$$

$$Nu_L = C (Ra_L)^n \quad (5)$$

In (5), the  $C$  and  $n$  constants depend on Rayleigh number range. This dimensionless number is defined by (6).

$$C = 0.59, n = 1/4 \text{ if } 10^4 \leq Ra_L \leq 10^9$$

$$C = 0.1, n = 1/3 \text{ if } 10^9 \leq Ra_L \leq 10^{13}$$

$$Ra_L = \frac{\beta g (\Delta T) L^3}{\nu \alpha} \quad (6)$$

Then, the convection heat transfer coefficient is calculated by (7), where  $k_f$  is the fluid thermal conductivity at  $T_f$ .

$$h = \frac{Nu_L k_f}{L} \quad (7)$$

The characteristic length  $L$ , used in (6) and (7), is the plate height for vertical flat plates.

#### Horizontal flat plates:

The correlation for the average Nusselt number is (5) and the  $C$  and  $n$  constants depend on the condition of the analyzed surface and the Rayleigh number range, calculated by (6).

For upper surface of hot plate or lower surface of cold plate [12].

$$C = 0.54, n = 1/4 \text{ if } 10^4 \leq Ra_L \leq 10^7$$

$$C = 0.15, n = 1/3 \text{ if } 10^7 \leq Ra_L \leq 10^{11}$$

For lower surface of hot plate or upper surface of cold plate [12].

$$C = 0.27, n = 1/4 \text{ if } 10^5 \leq Ra_L \leq 10^{10}$$

The convection heat transfer coefficient is calculated by (7). In (6) and (7), the characteristic length  $L$  is the relationship shown in (8).

$$L = \frac{\text{Area of horizontal plate}}{\text{Perimeter of horizontal plate}} \quad (8)$$

### III. RESULTS

#### External convection heat transfer coefficient, $h_{ex}$ .

The furnace gas temperature,  $T_{ge}$  is constant but the car body temperature,  $T_i$  changes from the initial value of 301 K to the equilibrium value near 460 K. For that reason, the film

temperature  $T_f$ , needed for estimation of gas thermo physical properties, is variable, so the Nusselt number and  $h_{ex}$  are variable along the furnace chamber. Gas properties are considered to be similar to air properties (Table I). Results are shown in Tables II to IV. Temperature dependant functions for  $h_{ex}$  are shown in Fig. 3 and these values were correlated in terms of the car body temperature (Table V), for being used in (2).

TABLE I  
AIR THERMOPHYSICAL PROPERTIES AT  $T_f$ , ( $T_{ge}=468K$ )

Ti (K)	Tf (K)	$\beta$ (1/K)	$\alpha$ (m <sup>2</sup> /s)	$\Delta T$ (K)	$\nu$ (m <sup>2</sup> /s)	K (W/mK)	Pr
303	385.5	0.002594	3.59E-05	165	2.48E-05	3.27E-02	0.6929
333	400.5	0.002496	3.83E-05	135	2.64E-05	3.38E-02	0.69
363	415.5	0.002406	4.11E-05	105	2.83E-05	3.49E-02	0.6888
393	430.5	0.002322	4.37E-05	75	3.00E-05	3.59E-02	0.6876
423	445.5	0.002244	4.64E-05	45	3.19E-05	3.70E-02	0.6864
453	460.5	0.002171	4.92E-05	15	3.37E-05	3.80E-02	0.6856

TABLE II  
EXTERNAL CONVECTION COEFF, VERTICAL FLAT PLATES, \* $L=0.68m$

Ti (K)	Tf (K)	$Ra_L$ (6)	$Nu_L$ (4)	$h_{ex}$ (W/m <sup>2</sup> K)
303	385.5	1.49E+09	138.4	6.65
333	400.5	1.03E+09	123.4	6.13
363	415.5	6.71E+08	108.2	5.55
393	430.5	4.09E+08	93	4.91
423	445.5	2.11E+08	76	4.13
453	460.5	6.05E+07	52.4	2.93

TABLE III  
EXTERNAL CONVECTION COEFFICIENT FOR FLOOR, \* $L=0.3m$  (8)

Ti (K)	Tf (K)	$Ra_L$ (6)	$Nu_L$ (5)	$h_{ex}$ (W/m <sup>2</sup> K)
303	385.5	1.28E+08	75.5	8.23
333	400.5	8.82E+07	66.8	7.52
363	415.5	5.76E+07	57.9	6.74
393	430.5	3.51E+07	49.1	5.89
423	445.5	1.81E+07	39.4	4.85
453	460.5	5.19E+06	25.8	3.27

TABLE IV  
EXTERNAL CONVECTION COEFFICIENT FOR ROOF, \* $L=0.3m$  (8)

Ti (K)	Tf (K)	$Ra_L$ (6)	$Nu_L$ (5)	$h_{ex}$ (W/m <sup>2</sup> K)
303	385.5	1.28E+08	28.7	3.13
333	400.5	8.82E+07	26.2	2.95
363	415.5	5.76E+07	23.5	2.74
393	430.5	3.51E+07	20.8	2.49
423	445.5	1.81E+07	17.6	2.17
453	460.5	5.19E+06	12.9	1.63

\*data provided by car manufacturer

TABLE V  
CORRELATION FOR EXTERNAL CONVECTIVE COEFFICIENT

Flat Plate	$h_{ex}$ (W/m <sup>2</sup> K)=f(Ti(K))	R <sup>2</sup>
Vertical	-8.333E-5Ti <sup>2</sup> +0.039Ti+2.448	0.9971
Floor	-1.069E-4Ti <sup>2</sup> +0.049Ti+3.201	0.9972
Roof	-4.444E-5Ti <sup>2</sup> +0.024Ti-0.0832	0.9954

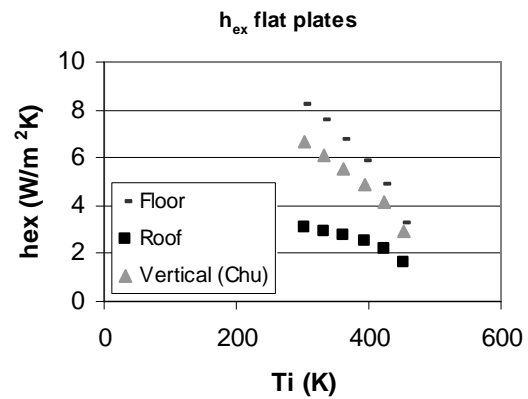


Fig.3. Flat plate  $h_{ex}$  vs car body temperature

#### Internal convection heat transfer coefficient, $h_{in}$ .

The internal gas temperature,  $T_{gi}$  is variable with the time and it is experimentally measured with a thermocouple as it is shown in Fig. 4. After approximately 9 minutes, the internal gas temperature reaches a stable value.

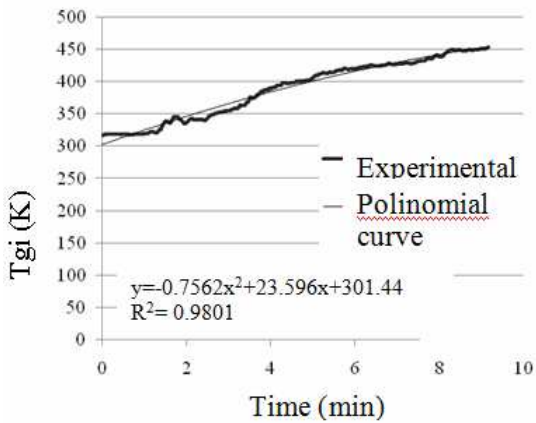


Fig.4. Internal gas temperature (Tgi) vs time

TABLE VI  
 AIR THERMOPHYSICAL PROPERTIES AT Tf, (Tgi VARIABLE)

Ti (K)	Tf (K)	$\beta$ (1/K)	$\alpha$ (m <sup>2</sup> /s)	$\Delta T$ (K)	$\nu$ (m <sup>2</sup> /s)	K (W/mK)	Pr
304	314	0.003185	2.46E-05	19.9	1.73E-05	2.73E-02	0.705
335	350	0.002857	2.99E-05	30.1	2.09E-05	3.00E-02	0.7
367	383.6	0.002607	3.54E-05	33.2	2.45E-05	3.25E-02	0.6934
403	416.1	0.002403	4.11E-05	26.2	2.83E-05	3.49E-02	0.6887
435	443.6	0.002254	4.60E-05	17.2	3.16E-05	3.68E-02	0.6866
450	455	0.002198	4.82E-05	10	3.30E-05	3.76E-02	0.6858

TABLE VII  
 INTERNAL CONVECTION COEFF, VERTICAL FLAT PLATES, L=0.68m

Ti (K)	Tf (K)	Ra <sub>L</sub> (6)	Nu <sub>L</sub> (4)	h <sub>in</sub> (W/m <sup>2</sup> K)
304	314	4.6E+08	96.7	3.89
335	350	4.23E+08	94.2	4.16
367	383.6	3.07E+08	85.3	4.08
403	416.1	1.67E+08	70.9	3.64
435	443.6	8.25E+07	57.4	3.11
450	455	4.26E+07	47.2	2.61

TABLE VIII  
 INTERNAL CONVECTION COEFFICIENT FOR FLOOR, L=0.3m (8)

Ti (K)	Tf (K)	Ra <sub>L</sub> (6)	Nu <sub>L</sub> (5)	h <sub>in</sub> (W/m <sup>2</sup> K)
304	314	3.95E+07	21.4	1.95
335	350	3.64E+07	21	2.1
367	383.6	2.64E+07	19.4	2.1
403	416.1	1.43E+07	16.6	1.93
435	443.6	7.08E+06	13.9	1.71
450	455	3.66E+06	11.8	1.48

TABLE IX  
 INTERNAL CONVECTION COEFFICIENT FOR ROOF, L=0.3m (8)

Ti (K)	Tf (K)	Ra <sub>L</sub> (6)	Nu <sub>L</sub> (5)	h <sub>in</sub> (W/m <sup>2</sup> K)
304	314	3.95E+07	51.1	4.66
335	350	3.64E+07	49.7	4.97
367	383.6	2.64E+07	44.6	4.84
403	416.1	1.43E+07	36.4	4.24
435	443.6	7.08E+06	27.9	3.42
450	455	3.66E+06	23.6	2.96

Here, Tf is also variable, so the Nusselt number and h<sub>in</sub> are variable along the furnace chamber. The air thermophysical properties are shown in Table VI. Results are shown in Tables VII to IX. Temperature dependant functions for h<sub>in</sub> are shown in Fig. 5 and these values were correlated in terms of the car body temperature (Table X), for being used in (2).

TABLE X  
 CORRELATION FOR INTERNAL CONVECTIVE COEFFICIENT

Flat Plate	h <sub>in</sub> (W/m <sup>2</sup> K)=f (Ti(K))	R <sup>2</sup>
Vertical	-1.381E-4Ti <sup>2</sup> +0.095Ti -12.353	0.9953
Roof	-1.706E-4Ti <sup>2</sup> +0.117Ti -14.98	0.9977
Floor	-6.566E-5Ti <sup>2</sup> +0.046Ti -6.083	0.9936

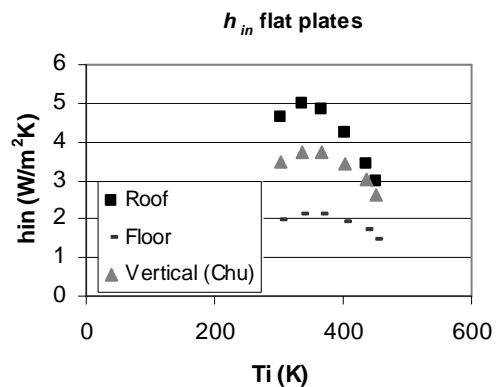


Fig. 5. Flat plate h<sub>B<sub>inB</sub></sub> vs car body temperature

*Biot numbers*

The maximum Biot number was calculated for each flat plate, using the highest value of the estimated convective coefficient. Biot values in Table XI are considerably lower than 0.1, so the lumped capacitance method is valid [13].

TABLE XI  
 MAXIMUM BIOT NUMBER ( $k=80.2 \text{ W/mK}$ )

Flat Plate	$h \text{ (W/m}^2\text{K)}$	Bi
Vertical	6.65	0.056
Roof	8.23	0.031
Floor	4.97	0.019

*Car body temperature*

The mathematical model shown in (2) was solved using the 4<sup>th</sup> order Runge- Kutta method and the temperature for each flat plate is compared with the experimental values (Figures 6 to 11).

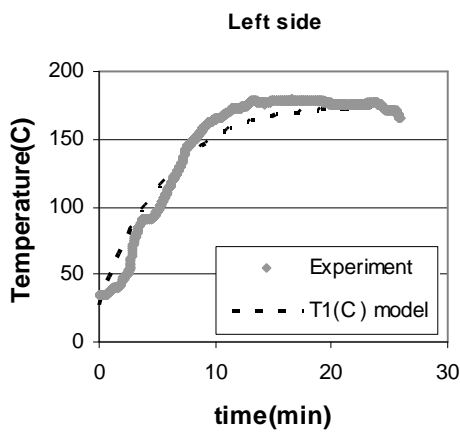


Fig.6. Left side, car body temperature vs time

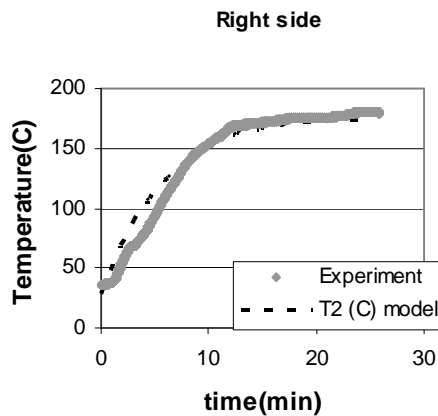


Fig.7. Right side, car body temperature vs time

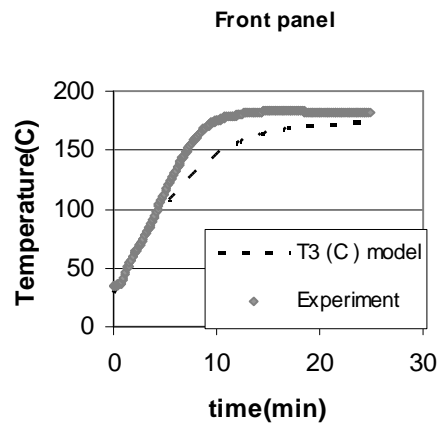


Fig.8. Front side, car body temperature vs time

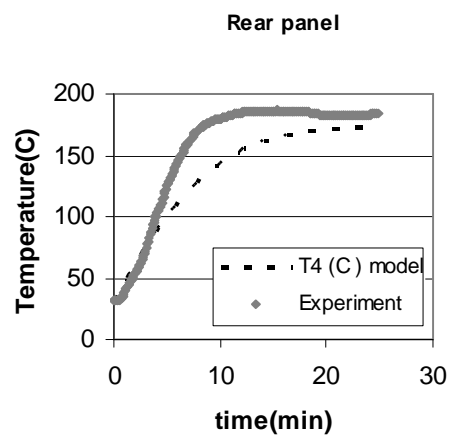


Fig. 9. Rear side, car body temperature vs time

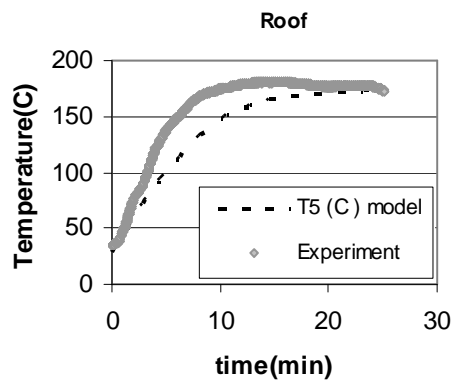


Fig.10. Roof, car body temperature vs time

In general, the model results are in good agreement with the trend in all the experimental curves. The highest deviation (4,7%) was found for the rear panel (Fig. 9) and the minimum deviation (1,4%) was for the floor (Fig. 11), calculated as in (9). These results validate the model and it can be used for evaluating furnace modifications.

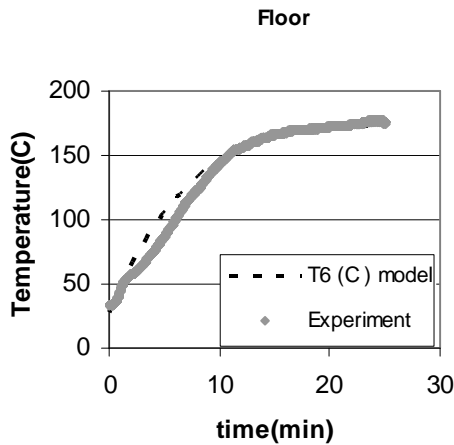


Fig.11. Floor, car body temperature vs time

APPENDIX  
 TABLE XII  
 GENERAL DATA

Absortivity, $\alpha$	0.101 <sup>a</sup>
Emissivity, $\epsilon$	0.88 <sup>a</sup>
Ca (J/kg K)	447 <sup>b</sup>
$\rho_a$ (kg/m <sup>3</sup> )	7870 <sup>b</sup>
$\sigma$ (W/m <sup>2</sup> K <sup>4</sup> )	$5.67 \cdot 10^{-8}$

<sup>a</sup> data provided by primer manufacturer

<sup>b</sup> data provided by car manufacturer

TABLE XIII  
 PARTICULAR DATA

Plate	1	2	3	4	5	6
	left	right	front	rear	roof	floor
Thickness (mm)	1	1	1.33	1.44	1	1.4
Initial T (K)	301	301	301	301	301	301

$$\% dev = \frac{\sum_{i=1}^n \left| \frac{(T(K))_i \text{ exp} - T(K)_i \text{ calc}}{T(K)_i \text{ exp}} \right|}{n} \times 100 \quad (9)$$

ACKNOWLEDGMENT

The authors thank to the engineers Romer Gutiérrez and Rafael Scovino for their help.

REFERENCES

[1] S. H. Han, S.W. Baek, S.H. Kang and C.Y. Kim. "Numerical analysis of heating characteristics of a slab in a bench scale reheating furnace", *Int. J. Heat Mass Transfer*, vol. 50 (9-10), 2007, pp.2019-2023.  
 [2] S.H. Han, S.W. Baek and M.Y. Kim. "Transient radiative heating characteristics of slabs in a walking beam type reheating furnace", *Int. J. Heat Mass Transfer*, vol. 52 (3-4), 2009, pp.1005-1011.

[3] M. Cuim, H. Chen, L. Xu and B. Wu. "Total heat exchange factor based on Non-Gray radiation Properties of Gas in reheating furnace", *Journal of Iron and Steel Research, International*, vol. 16 (3), 2009, pp.27-31.  
 [4] W.F. Wu, Y.H. Feng and X.X. Zhang. "Heat transfer analysis during rolling of thin slab in CSP", *Acta Metallurgica Sinica (English letters)*, vol. 19 (4), 2006, pp.244-250.  
 [5] A. Jaklic, F.Vode and T. Kolenko. "Online simulation model of the slab-reheating process in a pusher-type furnace", *Applied Thermal Engineering*, vol. 27 (5-6), 2007, pp.1105-1114.  
 [6] S. J. Barnett, M.N. Soutsos S.G. Millard and J.H. Bungey. "Strength development of mortars containing ground granulated blast-furnace slag: Effect of curing temperature and determination of apparent activation energies", *Cement and Concrete Research*, vol. 36 (3), 2006, pp.434-440.  
 [7] L. Zashkova. "Mathematical modelling of the heat behaviour in the ceramic chamber furnaces at different temperature baking curves", *Simulation Modelling Practice and Theory*, vol. 16 (10), 2008, pp.1640-1658.  
 [8] M.Y. Kim. "A heat transfer model for the analysis of transient heating of the slab in a direct-fired walking beam type reheating furnace". *International Journal of Heat and Mass Transfer, Volume 50, ( 19-20), 2007, pp. 3740-3748.*  
 [9] M.E. Masoumi, S.M. Sadrameli, J. Towfighi and A. Niaei. "Simulation optimization and control of a thermal cracking furnace". *Energy, Volume 31, (4), 2006, pp. 516-527.*  
 [10] S. W. Churchill and H.H.S. Chu, "Correlating equations for laminar and turbulent free convection from a vertical plate", *Int. J. Heat Mass Transfer*, vol. 18, 1975, pp.1323-1329.  
 [11] C.Y. Warner and V.S. Arpaci, "An experimental investigation of turbulent natural convection in air at low pressure along a vertical heated flat plate", *Int. J. Heat Mass Transfer*, vol. 11, 1968, pp.397-406.  
 [12] F. Incropera and D.P. DeWitt. *Fundamentos de Transferencia de Calor*. México: Prentice Hall, 1999, chapter 9.  
 [13] J. Pinto and N. Sánchez. *Rediseño de un horno para el curado de carrocería en una empresa ensambladora de vehículos*. Thesis, Mech. Eng. School, Universidad de Carabobo, Venezuela, may 2009.